Ain Shams Engineering Journal 14 (2023) 101840

Contents lists available at ScienceDirect

Ain Shams Engineering Journal

journal homepage: www.sciencedirect.com

Parametric analysis of the minimum cost design of flexible pavements

Primož Jelušič *, Rok Varga, Bojan Žlender

University of Maribor, Faculty of Civil Engineering, Transportation Engineering and Architecture, Smetanova 17, 2000 Maribor, Slovenia

ARTICLE INFO

Article history:
Received 14 March 2022
Revised 12 May 2022
Accepted 19 May 2022
Available online 09 June 2022

Keywords:
Pavement design
Optimization
Cost-optimization
Geosynthetics
Sensitivity analysis

ABSTRACT

This paper presents recommendations for an optimal pavement design. For this purpose, eight optimization models were developed, each corresponding to a different type of pavement. The optimization models were used to obtain the optimal designs for different design data. These results were used to perform a multi-parametric analysis, from which the design recommendations for an optimal design were derived. Since the optimization was performed for a large number of design-parameter combinations, the manual execution of the optimization algorithm was not feasible. Therefore, the optimization model was developed to include a loop to perform an optimization for each of the combinations. This study discusses the project data in which geosynthetically reinforced flexible pavements outperform conventional flexible pavements. In addition, the results of the study allow a direct comparison between geosynthetic reinforced and unreinforced flexible pavement structures once they are optimized.

© 2022 THE AUTHORS. Published by Elsevier BV on behalf of Faculty of Engineering, Ain Shams University. This is an open access article under the CC BY-NC-ND license (http://creativecommons.org/licenses/by-nc-nd/4.0/).

1. Introduction

Economic considerations are also taken into account in the design of flexible pavements when selecting the final layer thickness combinations and material properties that meet the design criteria. Therefore, multiple iterations must be performed to find a solution that meets the design requirements while minimizing construction costs. Pavement design methods vary in different countries around the world. Some are purely empirical, while others are mechanistic-empirical. The thickness of the base course with geosynthetics can be reduced without sacrificing performance, saving material and excavation, extending service-life and reducing long-term maintenance costs. Evaluations of the performance of geosynthetic-reinforced flexible pavements have been conducted using field tests, laboratory tests and numerical simulations [1]. Significant progress has been made in the field of geosynthetic reinforcement of pavements. In order to compare conventional flexible pavements with geosynthetic reinforced flexible pavements, both unreinforced and reinforced types of pavements should be optimized at minimum cost. For this purpose, optimization models should be developed and advanced algorithms should be applied.

Rouphail [2] applied the mixed integer linear programming model for flexible pavements to determine the number, type and thickness of pavement materials required to meet the structural strength requirements of pavement systems at minimum initial cost. The Star Pattern Search algorithm was used to obtain the minimum cost design of flexible and rigid pavements. Based on the optimization model, design graphs for the pavement design were developed to accelerate the selection of the most economical pavement type [3]. Both mentioned research papers are based on the AASHTO guidelines for pavement design. The genetic algorithm was applied to the problem of optimal design of rigid pavements by defining the total cost of the pavement materials as the objective function and considering all constraints that affected the design [4]. In the study conducted by Hadi and Arfiad [4], the optimization model was based on the AUSTROADS guidelines, and three main variables were considered, namely the thickness of the lean mixed concrete layer, the thickness of the bound material and the type of sub-base.

Pryke et al. [5] developed an optimization model and applied a genetic algorithm to minimize the pavement construction cost, where the design variables were the thickness of the pavement layers, the selection of the pavement materials and the number of layers within the pavement structure. The optimum pavement design and cost were compared for different traffic loads. The min-

* Corresponding author.
E-mail addresses: primoz.jelusic@um.si (P. Jelušič), rok.varga@um.si (R. Varga), bojan.zlender@um.si (B. Žlender).

Peer review under responsibility of Ain Shams University.

Production and hosting by Elsevier

https://doi.org/10.1016/j.asej.2022.101840
2090-4479/© 2022 THE AUTHORS. Published by Elsevier BV on behalf of Faculty of Engineering, Ain Shams University.
This is an open access article under the CC BY-NC-ND license (http://creativecommons.org/licenses/by-nc-nd/4.0/).

imum cost pavement design was also determined by direct and surrogate-based optimization approaches [6]. The required functional and structural performance criteria of the pavement design were assured by six distress reliabilities at the end of the service life of the pavement rather than by ASSHTO pavement design guidelines. The following distress reliabilities were considered: International Roughness Index (IRI), cracking of asphalt concrete at the surface, cracking of asphalt concrete from bottom to top, permanent deformation of asphalt concrete only and permanent deformation of the entire pavement. Several diagrams have also been developed in accordance with the Iran Highway Asphalt Paving Code Number to determine the optimum thickness of pavement layers, including asphalt concrete, granular base and granular subbase. These were dependent on road classification, design traffic and resilient modulus of the subgrade [7]. Based on 16 different alternatives for pavement design, Ghanizadeh [2-4] concluded that the base course can be removed from the optimal pavement design if the strength of the subgrade is increased. Tohidi et al. [8] compared the performance of the genetic algorithm and particle swarm optimization for determining the economically optimal pavement thickness and concluded that the genetic algorithm outperformed the particle swarm optimization. They also presented case studies on the effects of traffic changes on costs and the effects of CBR on cost reduction percentages. Based on the above studies, it can be concluded that the authors used various objective functions, constraints and optimization algorithms to enable optimal pavement designs.

The above researches [2-8] focused on minimizing the cost of pavement structures, but did not consider minimizing life-cycle costs. Mamlouk et al. [9] applied optimization methods for pavement management at the project level, where the optimization model included design guidelines, mechanistic-empirical performance models of pavements and a life cycle cost analysis. The developed optimization model allows for the calculation of the initial construction cost, overlay cost, highway user cost and the total pavement cost. Santos and Ferreira [10] performed 384 optimizations for different combinations of traffic load, foundation stiffness modulus and pavement structure to minimize pavement costs as applied to maintenance and rehabilitation strategies. Several researchers [11-14] have conducted studies looking at the design of optimal pavement structures based on life cycle costs. The studies have shown that life cycle cost is very important in the design and optimization of a pavement to get the optimal design. Zhang et al. [15] used dynamic programming optimization techniques to minimize the total life-cycle cost and environmental impact on pavement overlay systems. Lee et al. [16] reported that using optimization in pavement design that incorporates life cycle cost analysis can save up to 19% of costs. While the use of recycled concrete aggregate in the production of hot mix asphalt has a positive environmental impact, it could also have a significant effect on the mechanical properties, as reported by Sanchez-Cotte et al. [17].

One of the most important issues in pavement engineering is also the evaluation of the optimal timing for preventive maintenance measures for pavements under different traffic and climatic conditions [18]. Chong et al. [19] have developed an integrated approach for optimizing pavement life cycle and maintenance decisions. The rate of crack propagation that occurs with repeated loading in a hot mix asphalt layer was determined by Walubita et al [20] using several laboratory tests. The performance benefits of using interlayer grid reinforcement to mitigate reflective cracking in existing cracked pavements was presented by Walubita et al. [21].

There are many uncertainties in the design of pavement structures, namely traffic load, load distribution, environmental conditions, mechanical properties of soil and materials, and structural behavior. Therefore, reliability-based optimization models have been developed to account for these uncertainties [22-24]. Saride et al. [24] developed design charts for estimating reliability indexes against fatigue and rutting based damages on a wide range of pavement layer thicknesses and elastic moduli. Reliability-based design optimizations of asphalt pavements include not only the mechanical performance of the pavement, but also other aspects that have been shown to be relevant to the decision-making process [22].

In this work, the genetic algorithm was used to optimize a pavement structure according to the design guidelines for pavements [25]. It should be noted that the optimization model also allows for pavement variants with geosynthetic reinforcement, which was not yet considered in previous studies. Based on the developed optimization model, a parametric study was conducted for the optimal design of flexible pavement structures. Since the optimization was performed for a large number of design-parameter combinations, the manual execution of the optimization algorithm was not feasible. Therefore, an optimization model was developed to include a loop for performing optimizations for each of the combinations. In addition, an optimal pavement structure with geosynthetic reinforcement was included in the sensitivity analysis. Based on the sensitivity analysis, the selection of the optimal pavement type can be determined under certain traffic loads, climatic conditions and subgrade conditions.

2. Optimization model

In designing pavement structures, an engineer must start from the dimensions. This is not a trivial task, however, because ground conditions, traffic loads and other conditions are specific to each site. Even more difficult is the selection of appropriate dimensions that meet all the structural conditions with a minimal cost. Therefore, sections of the pavement structure need to be iteratively modified and structural conditions need to be rechecked. This iterative process can be performed by optimization algorithms capable of testing a large number of different pavement-structure sections in a short period of time. In order to apply optimization algorithms, a mathematical representation of the pavement structure design process must be defined. This is called an optimization model. In this optimization model, the cost objective function, geotechnical constraints and design constraints of a pavement structure are defined. It should be noted that this study provides an improved optimization model that takes into account not only structural-mechanic conditions, but also good design-practice conditions. Fig. 1 shows a cross section of eight different pavement structures. Each of these eight types of pavement structures were optimized for certain project data, therefore eight slightly modified optimization models were developed. The name of the pavement type was defined with two capital letters and two numbers. The letter B stands for the bound layers, U for the unbound layers and R for the geosynthetic reinforcement. The number 1 or 2 represent the number of bound layers (asphalt surface layer, asphalt base layer) or unbound layers (base course, sub-base course). The notation for the pavement type B2U2(R) defines a pavement that contains two bound layers and two unbound layers, as well as geosynthetic reinforcement. The cost objective functions for each pavement structure are presented in Table 1. The optimization model was built with the MATLAB [26] computer program and the real coded genetic algorithm [27] was applied to obtain optimal solutions.

In the equations (Eqs. 1.1–1.9) in Table 1, the unit price of the ground excavation is given by $c_{exe,re}$ (€/m^3); c_{gc} (€/m^2) is the unit price of the ground compaction; $c_{fill,sb}$ (€/m^3) is the unit price of the unbound sub-base fill; $c_{fill,b}$ (€/m^3) is the unit price for unbound base fill, which is a higher quality material than the unbound sub-base fill; $c_{as,subs}$ (€/m^2) is the price of the asphalt substrate; c_{as} (€/m^3) is the price of the asphalt surface layer; c_{ab} (€/m^3) is the unit

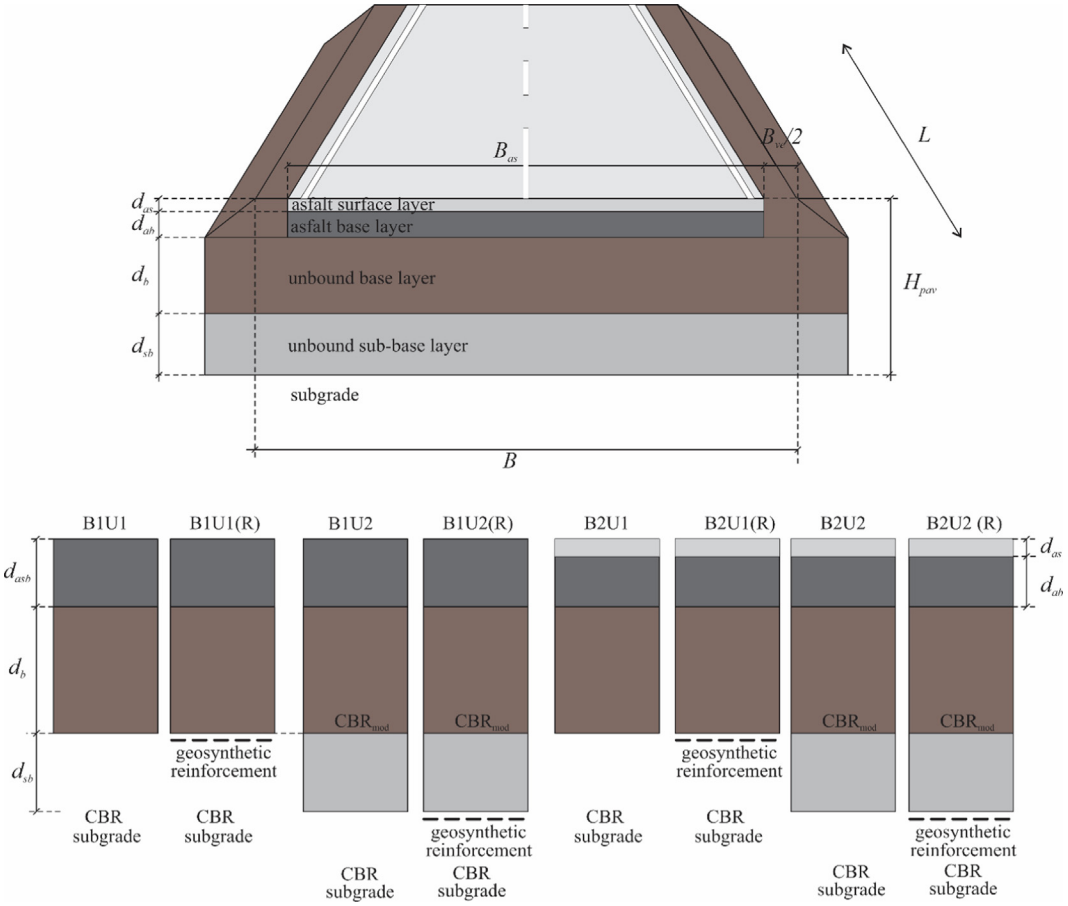

Fig. 1. Geometry and parameters of the pavement structure.

Table 1
The cost objective functions of the pavement structure.

The cost objective functions of a pavement structure	*TYPE*	Eq.
$COST_{pav} = C_{exc,re} + C_{gc} + C_{fill,b} + C_{as,subs} + C_{fill,sb} + C_{as} + C_{ab} + C_{geo}$	B2U2(R)	(1)
$COST_{pav} = C_{exc,re} + C_{gc} + C_{fill,b} + C_{as,subs} + C_{asb}$	B1U1	(1a)
$COST_{pav} = C_{exc,re} + C_{gc} + C_{fill,b} + C_{as,subs} + C_{asb} + C_{geo}$	B1U1(R)	(1b)
$COST_{pav} = C_{exc,re} + C_{gc} + C_{fill,b} + C_{as,subs} + C_{asb} + C_{fill,sb}$	B1U2	(1c)
$COST_{pav} = C_{exc,re} + C_{gc} + C_{fill,b} + C_{as,subs} + C_{asb} + C_{fill,sb} + C_{geo}$	B1U2(R)	(1d)
$COST_{pav} = C_{exc,re} + C_{gc} + C_{fill,b} + C_{as,subs} + C_{as} + C_{ab}$	B2U1	(1e)
$COST_{pav} = C_{exc,re} + C_{gc} + C_{fill,b} + C_{as,subs} + C_{as} + C_{ab} + C_{geo}$	B2U1(R)	(1f)
$COST_{pav} = C_{exc,re} + C_{gc} + C_{fill,b} + C_{as,subs} + C_{fill,sb} + C_{as} + C_{ab}$	B2U2	(1g)
$C_{exc,re} = c_{exc,re} \cdot h_{total} \cdot (B_{ve} + B_{as})$	Ground excavation	(1.1)
$C_{gc} = c_{gc} \cdot (B_{ve} + B_{as})$	Ground compaction	(1.2)
$C_{fill,b} = c_{fill,b} \cdot (B_{ve} + B_{as}) \cdot d_b$	Base-layer fill	(1.3)
$C_{as,subs} = c_{as,subs} \cdot B_{as}$	Asphalt substrate	(1.4)
$C_{fill,sb} = c_{fill,sb} \cdot (B_{ve} + B_{as}) \cdot d_{sb}$	Sub-base fill	(1.5)
$C_{as} = c_{as} \cdot B_{as} \cdot d_{as}$	Asphalt surface layer	(1.6)
$C_{ab} = c_{ab} \cdot B_{as} \cdot d_{ab}$	Asphalt base layer	(1.7)
$C_{geo} = c_{geo} \cdot (B_{ve} + B_{as})$	Geosynthetic installation	(1.8)
$C_{asb} = c_{asb} \cdot B_{as} \cdot d_{asb}$	Single asphalt layer	(1.9)

price of the asphalt base layer and c_{geo} (€/m^2) represents the price of the geosynthetics. The denotation c_{asb} (€/m^3) is used in cases where the type of pavement consists of only one asphalt layer. Furthermore, B (m) represents the width of the pavement structure, while B_{ve} and B_{as} represent the width of the verge and the asphalt surface, respectively; and h_{total} (m) is the total thickness of the pavement structure. The optimization model consists of four different variables which represent the different layers of a pavement structure. The variable d_{as} (m) represents the asphalt surface layer, d_{ab} (m) represents the base layer of the asphalt, the unbound base layer is represented by d_b (m), the unbound sub-base layer is represented by the variable d_{sb} (m), while the pavement structure construction cost is defined as $COST_{pav}$ (EUR/m). The variable d_{asb} (m) is used in pavement types that include only a single layer of asphalt.

2.1. Design conditions built into the optimization model

The geotechnical analysis and the dimensioning conditions restrain the cost objective function. This is done to make sure that the conditions for the design are in accordance with the required recommendations. The trend in pavement design is toward mechanical-empirical (M−E) design methods [28]. However, in European countries, empirical methods are still prescribed for pavement design and are widely used in engineering practice. In the presented analyses, the empirical method AASHTO was used for the pavement design, based on the number of equivalent single axle loads (ESAL) caused by travelling on the road pavement in the design life. It is based on the following experimentally obtained parameters, including: annual average daily traffic in the first year of the design life, factors that consider the division of traffic into directions and lanes, overall conversion factor of the total passages of different heavy vehicle axles into ESALs, heavy vehicle annual growth rate and design life in years. ESAL is the input data in this model and is determined by applying local technical specifications for roads [25], based on AASHTO [29] and European guidelines. Nine different conditions were defined according to the flexural pavement design guidelines. These conditions had to be met to ensure a sufficient design. Eight different pavement structures were analyzed, and the conditions had to be adapted for each type of pavement structure. The list of equations that are included in each pavement optimization model are given in Table 2.

Condition 1 is satisfied when the calculated pavement thickness-index (D_{total}) is greater than the required pavement thickness-index (D_{req}) [25], see Eq. (2):

$$D_{total} \geq D_{req} \tag{2}$$

The pavement thickness-index D_{total} is defined as:

$$D_{total} = d_{as} \cdot a_{i,as} + d_{ab} \cdot a_{i,ab} + d_b \cdot a_{i,b} \quad \text{or} \tag{2.1a}$$

$$D_{total} = d_{asb} \cdot a_{i,asb} + d_b \cdot a_{i,b} \tag{2.1b}$$

In the case where two layers of asphalt were used (asphalt surface layer and asphalt base layer), Eq. (2.1a) was employed and Eq. (2.1b) was used for single asphalt layers. The equivalence factors $a_{i,as}$, $a_{i,ab}$ and $a_{i,b}$ are shown in Table 3. The required thickness of the asphalt, based on the guidelines, is represented with $d_{asb,0}$ (cm) and was calculated with Eq. (2.2):

$$d_{asb,0} = a_1 \cdot T_n^{\,a_2} \tag{2.2}$$

The constants a_1 and a_2 are shown in Table 3. The number of ESALs T_n was determined based on several items that consider equivalent daily traffic, cross section of pavement, lane width, longitudinal tilt of the pavement, additional dynamic loading and growth of traffic during the pavement's lifetime. According to the guidelines [25], the required pavement thickness-index was determined as:

$$D_{req} = d_{asb,0} \cdot 0.38 + d_{b,CBR_{mod}} \cdot 0.14 \quad \text{or} \tag{2.3a}$$

$$D_{req} = d_{asb,0} \cdot 0.38 + d_{b,CBR} \cdot 0.14 \tag{2.3b}$$

Eq. (2.3a) was used when the pavement structure included an unbound base layer and an unbound sub-base layer. The main aim of including the sub-base layer was to increase the CBR. The required thickness of the unbound base layer $d_{b,CBR}$ depended on the CBR of the subgrade and was calculated with Eq. (2.4a):

$$d_{b,\mathrm{CBR}} = (c_1 - c_2 \cdot CBR) \cdot \ln(T_n) - c_3 + e^{(c_4 \cdot CBR) \cdot c_5} \tag{2.4a}$$

The CBR of the subgrade can be improved to $\mathrm{CBR_{mod}}$ by adding an unbound sub-base fill. In this case, the required thickness of the unbound base layer $d_{b,CBRmod}$, see Eq. (2.4b):

$$d_{b,CBR_{mod}} = (c_1 - c_2 \cdot CBR_{mod}) \cdot \ln(T_n) - c_3 + e^{(c_4 \cdot CBR_{mod}) \cdot c_5} \tag{2.4b}$$

Moreover, if geosynthetic reinforcement is provided, the thickness of the unbound base layer can be further reduced, see Eq. (2.4c):

$$d_{b,CBR} = \left((c_1 - c_2 \cdot CBR) \cdot \ln(T_n) - c_3 + e^{(c_4 \cdot CBR) \cdot c_5}\right) / \gamma_{geo,b} \quad \text{or} \tag{2.4c}$$

$$d_{b,CBR_{mod}} = \left((c_1 - c_2 \cdot CBR) \cdot \ln(T_n) - c_3 + e^{(c_4 \cdot CBR) \cdot c_5}\right) / \gamma_{geo,b} \tag{2.4d}$$

Geosynthetic reinforcement increases the bearing capacity of the subgrade and stiffens the base course by limiting the lateral movement of both the base course material and the subgrade. These improvements in the pavement's structure were due to geosynthetic reinforcement. They were considered in terms of reducing the base course thickness ($\gamma_{geo,b}$) and were based on laboratory tests, field tests and theory-based design methods [1,30-33]. The constants c_1, c_2, c_3, c_4, c_5 and $\gamma_{geo,b}$ are provided in Table 3. The constants c_1, c_2, c_3, c_4 and c_5 were determined using a curve fit

Table 2
List of conditions included in each type of pavement structure.

	B1U1	B1U1(R)	B1U2	B1U2(R)	B2U1	B2U1(R)	B2U2	B2U2(R)
Objective Function	Eq. (1a)	Eq. (1b)	Eq. (1c)	Eq. (1d)	Eq. (1e)	Eq. (1f)	Eq. (1g)	Eq. (1)
Condition 1Eq. (2)	Eq. (2.1b)	Eq. (2.1b)	Eq. (2.1b)	Eq. (2.1b)	Eq. (2.1a)	Eq. (2.1a)	Eq. (2.1a)	Eq. (2.1a)
	Eq. (2.2)	Eq. (2.2)	Eq. (2.2)	Eq. (2.2)	Eq. (2.2)	Eq. (2.2)	Eq. (2.2)	Eq. (2.2)
	Eq. (2.3b)	Eq. (2.3b)	Eq. (2.3a)	Eq. (2.3a)	Eq. (2.3b)	Eq. (2.3b)	Eq. (2.3a)	Eq. (2.3a)
	Eq. (2.4a)	Eq. (2.4c)	Eq. (2.4b)	Eq. (2.4d)	Eq. (2.4a)	Eq. (2.4c)	Eq. (2.4b)	Eq. (2.4d)
Condition (2) Eq. (3)	Eq. (3.1b)	Eq. (3.1b)	Eq. (3.1b)	Eq. (3.1b)	Eq. (3.1a)	Eq. (3.1a)	Eq. (3.1a)	Eq. (3.1a)
Condition (3) Eq. (4)	Eq. (4.1a)	Eq. (4.1a)	Eq. (4.1b)	Eq. (4.1b)	Eq. (4.1a)	Eq. (4.1a)	Eq. (4.1b)	Eq. (4.1b)
Condition (4) Eq. (5)	Eq. (5.1b)	Eq. (5.1b)	Eq. (5.1c)	Eq. (5.1c)	Eq. (5.1b)	Eq. (5.1d)	Eq. (5.1a)	Eq. (5.1a)
	Eq. (5.2)	Eq. (5.2)	Eq. (5.2)	Eq. (5.2)	Eq. (5.2)	Eq. (5.2)	Eq. (5.2)	Eq. (5.2)
Condition (5) Eq. (6))	N/A	N/A	Eq. (6.1a)	Eq. (6.1b)	N/A	N/A	Eq. (6.1a)	Eq. (6.1b)
Condition (6) Eq. (7))	N/A	N/A	N/A	N/A	Eq. (7)	Eq. (7)	Eq. (7)	Eq. (7)
Condition (7) Eq. (8)	N/A	N/A	N/A	N/A	Eq. (8)	Eq. (8)	Eq. (8)	Eq. (8)
Condition (8) Eq. (9)	Eq. (9)	Eq. (9)	Eq. (9)	Eq. (9)	N/A	N/A	N/A	N/A
Condition (9) Eq. (10)	Eq. (10)	Eq. (10)	Eq. (10)	Eq. (10)	Eq. (10)	Eq. (10)	Eq. (10)	Eq. (10)
Condition10 Eq. (11)	N/A	N/A	Eq. (11)	Eq. (11)	N/A	N/A	Eq. (11)	Eq. (11)

Table 3
Input data for the optimization model.

$c_{exe,re}$ (€/m^2)	9	$a_{i,as}$	0.42	c_2	0.376
c_{gc} (€/m^2)	2.5	$a_{i,ab}$	0.35	c_3	26.64
$c_{fill,sb}$ (€/m^3)	24	$a_{i,b}$	0.14	c_4	0.141
$c_{fill,b}$ (€/m^3)	36	$a_{i,asb}$	0.35	c_5	4.882
$c_{as,subs}$ (€/m^2)	1.5	a_1	0.6567	CBR_{mod} (%)	15.0
c_{as} (€/m^3)	300	a_2	0.2175	$\gamma_{geo,b}$	1.5
c_{ab} (€/m^3)	200	b_1	8.382	$\gamma_{geo,sb}$	2.0
c_{asb} (€/m^3)	250	b_2	−0.791	$d_{as,min}$ (m)	0.04
c_{geo} (€/m^2)	3.2	b_3	1.975	$d_{ab,min}$ (m)	0.06
B_{ve} (m)	1	b_4	1.912	$d_{asb,min}$ (m)	0.08
B_{as} (m)	8	c_1	6.239	$d_{b,min}$ (m)	0.25
				$d_{sb,min}$ (m)	0.20

of the guidelines [25,29] for the required asphalt thickness and the unbound base layer based on ESAL. The goodness of fit of the curve fit is determined by R^2 and RMSE and results in 0.987 and 1.418 cm, respectively.

Condition (2) describes the required asphalt layer thickness. The provided thickness of the asphalt layer must be greater or equal to $d_{asb,0}$, as shown in Eq. (3).

$$d_{prov} \geq d_{asb,0} \tag{3}$$

$$d_{prov} = d_{as} + d_{ab} \quad \text{or} \tag{3.1a}$$

$$d_{prov} = d_{asb} \tag{3.1b}$$

Eq. (3.1b) is valid for pavement structures where only a single quality of asphalt layer is used, while Eq. (3.1a) considers the asphalt surface layer and the asphalt base layer.

Condition (3), shown below, is described with Eq. (4) and provides the required thickness of the unbound base layer.

$$d_b \geq d_{b,req} \tag{4}$$

where

$$d_{b,req} = d_{b,CBR} \quad \text{or} \tag{4.1a}$$

$$d_{b,req} = d_{b,CBR_{mod}} \tag{4.1b}$$

Condition (4) is the condition for frost resistance. Eq. (5) describes the relationship required to satisfy the longevity of the pavement structure.

$$h_{total} \geq h_{req} \tag{5}$$

where h_{total} is the total thickness of the pavement structure. While four different layer configurations in the pavement structure were analysed, only one of the appropriate total thicknesses was calculated with the following equations:

$$h_{total} = d_{as} + d_{ab} + d_b + d_{sb} \tag{5.1a}$$

$$h_{total} = d_{asb} + d_b \tag{5.1b}$$

$$h_{total} = d_{asb} + d_b + d_{sb} \tag{5.1c}$$

$$h_{total} = d_{as} + d_{ab} + d_b \tag{5.1d}$$

The required thickness of the pavement structure is defined with Eq. (5.2). The factor f_{fr} was determined based on the guidelines [25]. The value f_{fr} represents the conditions of the material at the site: the hydrologic conditions and the elevation of the site. Hydrologic conditions are favourable when the road embankment is at least 1.5 m high, the groundwater level is constantly lower than the freezing depth h_m, the excavation pit is well drained, and the inflow of water into the road is prevented. Different combinations of these conditions resulted in four different f_{fr} values. These values are listed in Table 4. f_{fr} is referred to as the site condition in this model. Moreover, the value of h_m was evaluated based on geographical location, since the parameter represents the depth of the freezing point at that location.

$$h_{req} = h_m \cdot f_{fr} \tag{5.2}$$

Condition (5) constrains the minimum thickness of the unbound sub-base layer by Eq. (6).

$$d_{sb} \geq d_{sb,CBR_{mod}} \tag{6}$$

The minimal required unbound sub-base layer for a specific CBR value (CBR_{mod}) was calculated using Eq. (6.1a) or Eq. (6.1b) in cases when geosynthetic reinforcement was included between the subgrade and the unbound sub-base layer.

$$d_{sb,CBR_{mod}} = b_1 \cdot \left(\frac{b_2 \cdot (CBR_{mod} - CBR)}{b_3 - CBR} + b_4 \right) \tag{6.1a}$$

$$d_{sb,CBR_{mod}} = \left(b_1 \cdot \left(\frac{b_2 \cdot (CBR_{mod} - CBR)}{b_3 - CBR} + b_4 \right) \right) / \gamma_{geo,sb} \tag{6.1b}$$

The constants b_1, b_2, b_3 and b_4 were determined using a curve fit of the guidelines [25] for the required sub–base thickness to achieve an improved CBR_{mod} of subgrade. The goodness of fit of the curve fit is determined by R^2 and RMSE and results in 0.9599 and 2.571 cm, respectively. The minimum thickness of each layer in the pavement structure was also limited with four additional conditions. Condition (6) defines the minimum thickness of the asphalt surface layer (see Eq. (7)), and condition (7) limits the minimum thickness of the asphalt base layer (see Eq. (8)). In cases where the pavement structure was constructed with a single asphalt layer, the minimum thickness was defined with condition (8) (see Eq. (9)). The minimum thickness of the unbound base layer and the minimum thickness of the unbound sub-base layer are expressed with conditions (9) (see Eq. (10)) and condition (10) (see Eq. (11)), respectively.

Table 4
Minimum required thicknesses of the pavement structures h_{req} [25].

Resistance of the material under the pavement structure against the effects of freezing and thawing	Hydrological Conditions	Minimum thickness of pavement structure $h_{req} = (f_{fr}) \cdot h_m$ h_m is depth of frost penetration	
		to an altitude of 600 m	from an altitude of 600 m
resistant	favourable	$(0.6) \cdot h_m$	$(0.7) \cdot h_m$
	unfavourable	$(0.7) \cdot h_m$	$(0.8) \cdot h_m$
not resistant	favourable	$(0.7) \cdot h_m$	$(0.8) \cdot h_m$
	unfavourable	$(0.8) \cdot h_m$	$(0.9) \cdot h_m$

$$d_{as} \geq d_{as,min} \tag{7}$$

$$d_{ab} \geq d_{ab,min} \tag{8}$$

$$d_{asb} \geq d_{asb,min} \tag{9}$$

$$d_{b} \geq d_{b,min} \tag{10}$$

$$d_{sb} \geq d_{sb,min} \tag{11}$$

Since not all equations apply to every defined pavement type, Table 2 defines the equations included in the optimization model. For example, pavement type B1U1 includes Conditions (1)–(4) and Conditions (8)–(9) defined by equations 2.1b, 2.2, 2.3b, 2.4a, 3.1b, 4.1a, 5.1b, 5.2, 9, and 10.

3. Multi-parametric analysis

The optimization model presented above was developed in a general form so that an optimal design for a pavement structure can be obtained for any project data (e.g. subgrade properties, traffic loads, climate zones…). A series of optimizations for the pavement structure were performed for a combination of different parameters, i.e. different values of the total number of ESALs T_n. ESAL was fixed at specific values in the multiparametric analysis and is fixed in the optimization process (T_n;$1 \cdot 10^4$; $1 \cdot 10^5$; $1 \cdot 10^6$; $1 \cdot 10^7$; $1 \cdot 10^7$). California Bearing Ratios *CBR*, depths of frost penetration h_m and site conditions f_{fr}. The optimization process was repeated eight times, while eight different pavements structures were compared in terms of costs. Input data, variables and a cost objective function subjected to (in)equality geotechnical and design constraints were included in the model. An optimal cost and an optimal dimension of the pavement's structure were determined for each optimization. An RCGA was used to solve the optimization problems [27]. A parametric optimization was performed for all 3200 combinations of the following different design parameters:

- eight different pavement structures: *TYPE* (B1U1, B1U1(R), B1U2, B1U2(R), B2U1, B2U1(R), B2U2, B2U2(R))
- total number of ESALs: T_n ($1 \cdot 10^4$; $1 \cdot 10^5$; $1 \cdot 10^6$; $1 \cdot 10^7$; $1 \cdot 10^7$)
- California Bearing Ratio: *CBR* (3%; 4%; 5%; 6%; 7%)
- depth of frost penetration: h_m (40 cm; 60 cm; 80 cm; 100 cm)
- conditions of the material at the site and the hydrological conditions: f_{fr} (0.6; 0.7; 0.8; 0.9)

The input data used in the optimization model are shown in Table 3 and remained constant in the multiparametric analysis. In order to make the results useful for different widths of pavement structures, the optimal cost $COST_{pav}$ was normalized with the asphalt pavement width B_{as} and the verge width B_{ve}. This was done to obtain the optimal cost of the paved structure with the asphalt layer $Cost_{as}$ (EUR/m^2) and the related cost of the verge $Cost_{ve}$ (EUR/m^2).

$$Cost_{as} = c_{exc,re} \cdot h_{total} + c_{gc} + c_{fill,b} \cdot d_b + c_{as,subs} + c_{fill,sb} \cdot d_{sb} + c_{as} \cdot d_{as} + c_{ab} \cdot d_{ab} + c_{geo} \tag{12}$$

$$Cost_{ve} = c_{exc,re} \cdot h_{total} + c_{gc} + c_{fill,b} \cdot d_b + c_{fill,sb} \cdot d_{sb} + c_{geo} \tag{13}$$

Since the optimizations had to be performed for each combination of design parameters, manual execution of the optimization algorithm was not feasible. Therefore, an optimization model was developed that included a loop to perform an optimization for each of the 3200 combinations. The total time to obtain the optimal solutions for all the defined combinations was about 35 h.

Fig. 2 shows the optimal results for a pavement structure that is constructed on a sub-grade with *CBR* = 3% and in a climate zone where the depth of frost penetration is h_m = 100 cm; the site conditions correspond to f_{fr} = 0.8. With the help of these diagrams, it is possible to determine the optimal thicknesses of the pavement layers (d_{as}, d_{ab}, d_{asb}, d_b and d_{sb}) and which type of pavement structure produces the minimum construction cost at different traffic loads. Each line in these diagrams presents the optimal solution for different types of pavements. Fig. 2a clearly shows that the optimal type of pavement changes with the total number of ESALs. With small traffic loads ($1 \cdot 10^4$), the optimal pavement type is B2U2(R); with medium traffic loads ($1 \cdot 10^6$), it is B1U1 and with large traffic loads ($1 \cdot 10^8$), the optimal solution is to construct a B2U1(R) type pavement. Fig. 2b shows the unit cost for the verge of pavement. The degree of utilization of condition 1 ($u_{load} = D_{req}/D_{total}$) is presented in Fig. 2c. The optimal thickness of each layer of pavement structure can be obtained from Fig. 2d-2f. The upper curve in Fig. 2f represents the optimal thickness of the asphalt layer d_{asb}. The bottom curve represents the optimal thickness of the asphalt base layer d_{ab}. It should be noted that for all parameter combinations, the optimum thickness of the asphalt surface layer was calculated to be d_{as} = 4 cm, which is the minimum value specified.

The optimal solutions for a pavement structure that is constructed on a sub-grade with *CBR* = 7% (h_m = 100 cm and f_{fr} = 0.8) are presented in Fig. 3. In this case, with small traffic loads ($1 \cdot 10^4$), the optimal pavement type is B1U2; with medium traffic loads ($1 \cdot 10^6$), it is B1U1 and with large traffic loads ($1 \cdot 10^8$), the optimal solution is to construct a B2U2 type pavement. While the optimal asphalt thickness is completely dependent on the total number of ESALs, the optimal asphalt thickness of any type of pavement can be determined from Fig. 4.

Fig. 2 and Fig. 3 also show substantial differences in pavement cost for different pavement types, even though each pavement type was optimized. The optimal cost at 10^8 load transitions of pavement type B1U2 yields 133.87 EUR/m^2, while the optimal pavement type B2U1(R) yields only 111.14 EUR/m^2, which is about 20% less than the B1U2 pavement.

Among 3200 optimal solutions for different combinations of parameters, an optimal type of pavement structure was found with a minimum cost along with the pavement's layer-dimensions. This reduction provided 400 results. Only the most economical type of pavement was selected from 8 different optimized pavements. Table 5 presents 25 optimal solutions that were obtained for a depth of frost penetration of h_m = 100 cm with site conditions at f_{fr} = 0.8. Table 5 clearly shows that at CBR = 3% the pavement structure with geosynthetic reinforcement is the most economical, while at a larger CBR = 7%, the optimal pavements do not include geosynthetic reinforcement. The multi parametric analysis also shows that each pavement type defined in this paper was found to be optimal for certain input data, see Fig. 5.

Fig. 6 shows the results of optimizations that include information about optimal pavement types, optimal thicknesses of unbound bases and unbound subbase layers. It should be noted that numerical values are assigned to each pavement type (1 - B1U1, 2 - B1U2, 3 - B2U1, 4 - B2U2, 5 - B1U1(R), 6 - B1U2(R), 7 - B2U1(R), 8 - B2U2(R)). For very unfavorable site conditions (f_{fr} = 0.9), pavement types B2U1(R) and B2U2(R) predominate and show that geosynthetic reinforcement at the base or subbase layer is required if the CBR value of the subgrade is low (CBR = 3%). When the CBR of the subgrade is high, the need of geosynthetic reinforcement decreases and pavement types B1U2 and B2U2 prove to be the most economically efficient. With increasing ESAL, the need for base layers also increases. This is necessary in order to achieve the required pavement thickness-index, which can be seen by a decrease in the required thickness of the sub-base layer.

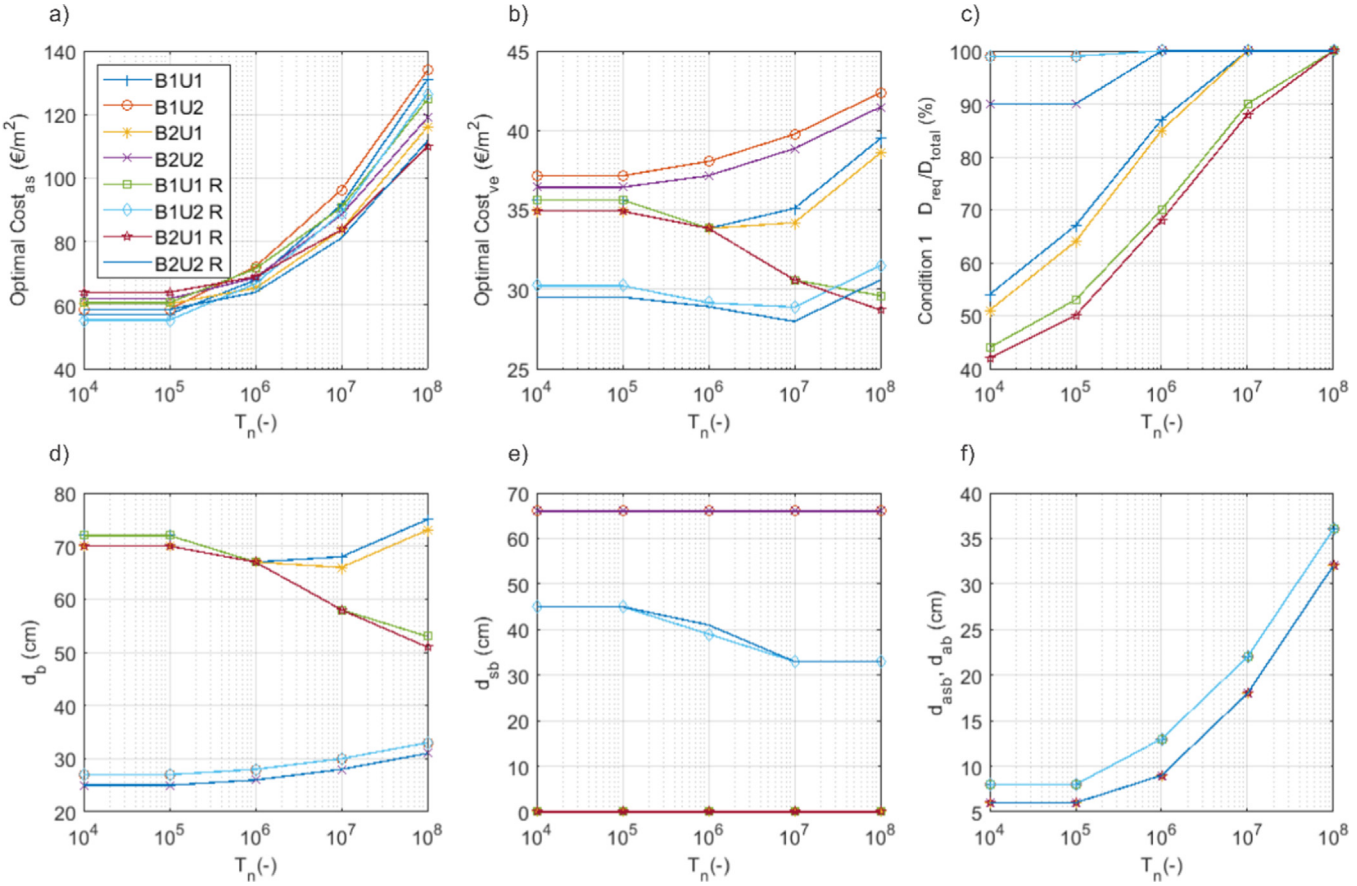

Fig. 2. Optimal solution for *CBR* = 3%, depth of frost penetration h_m = 100 cm and site conditions f_{fr} = 0.8.

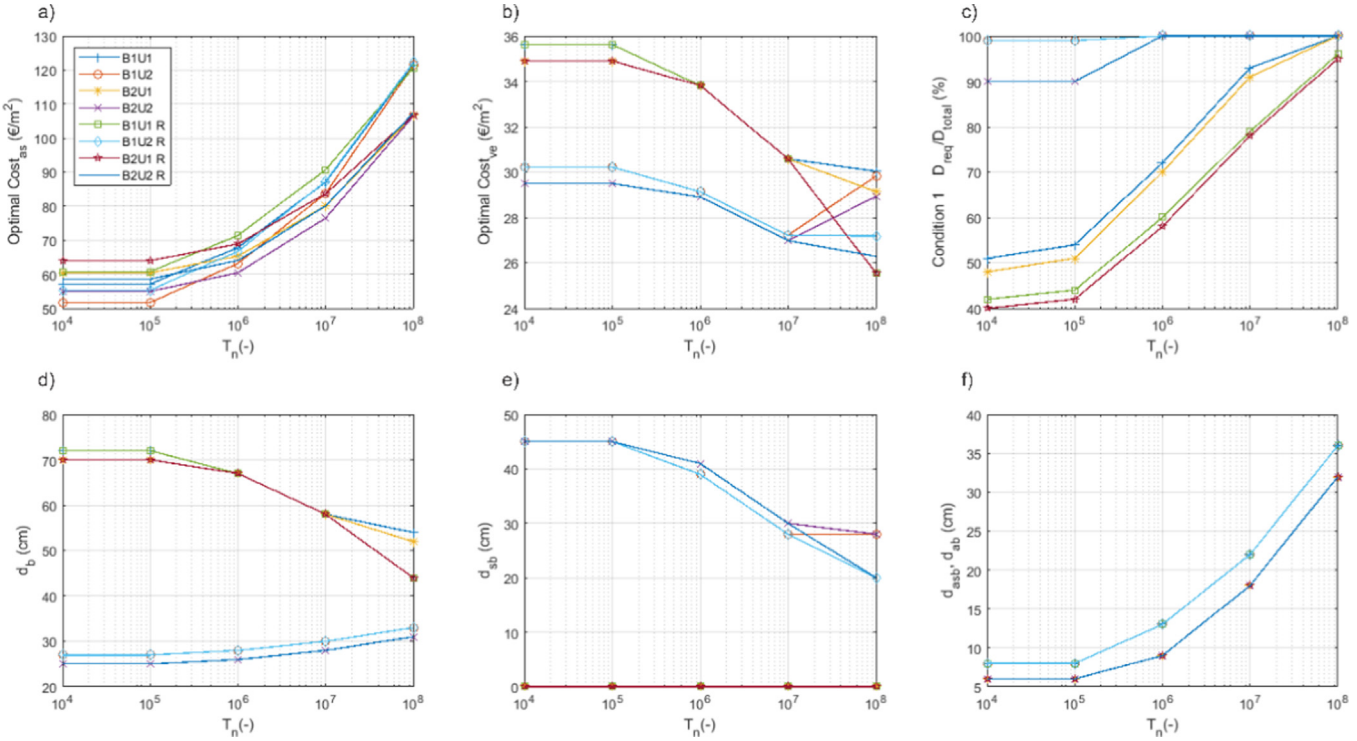

Fig. 3. Optimal solution for *CBR* = 7%, depth of frost penetration h_m = 100 cm and site conditions f_{fr} = 0.8.

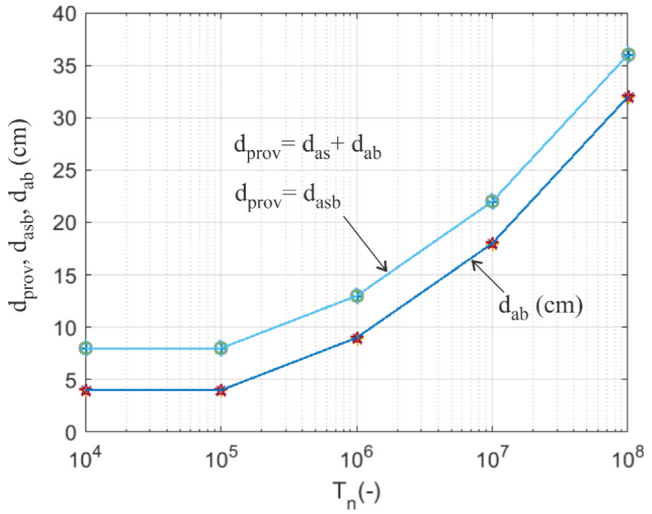

Fig. 4. Optimal thickness of a provided asphalt layer d_{prov} and the optimal thickness of an asphalt base layer d_{ab}.

For unfavorable site conditions (f_{fr} = 0.8), the results are presented in Fig. 7. When the required freezing depth h_m is high, pavement type B2U2(R) is optimal because the sub-base layer provides the required frost resistance at a lower cost. When the freezing depth becomes shallower, the optimal pavement type changes to B2U1(R), where only the base layer provides the required thickness for both freezing and pavement thickness-index conditions. Pavement type B2U1(R) was predominant for almost all subgrade CBR values when the required freezing depth became shallower. As the freezing depth becomes shallower, the sub-base layer requirement decreases and the pavement thickness-index condition becomes more critical. This can be seen by the increase in the thickness of the base layer to satisfy the pavement thickness-index condition. The optimal solutions for the remaining factors f_{fr} = 0.7 and 0.6 are presented in Table 6 and 7, respectively.

4. Sensitivity analysis

The optimal design of the pavement structure was determined for different input data. The four main input data are the total number of ESAL (T_n), the California Bearing Ratio (*CBR*), the depth of frost penetration (h_m) and the site conditions (f_{fr}). The main objective of this multiparametric analysis was to use these main attributes to predict other continuous attributes, such as the optimal cost of the pavement structure ($Cost_{as}$), the optimal pavement type (TYPE), the total thickness of asphalt layer (d_{asb} or d_{as} plus d_{ab}) and the total thickness of the unbound layer (d_b + d_{sb}). Before applying the predictive model, the dataset was divided into a training dataset (odd indexed samples) and a checking dataset (even indexed samples). The "exhsrch" function included in MATLAB was used to perform an exhaustive search within the available inputs to select the set of inputs that have the greatest impact on the optimal cost of the pavement structure and the thickness of layers. For the "exhsrch" function, the predictive models were built for each parameter combination and trained for an epoch; the achieved performance was then reported. The leftmost input variable in Fig. 8 is the most relevant in terms of output, while it has the lowest root-mean-square error (RMSE). The RMSE is defined as follows:

$$RMSE = \sqrt{\frac{\sum_{i=1}^{n}\left(\hat{x}_i - x_i\right)^2}{n}} \tag{14}$$

where $\hat{x}_i$ are the predicted values and x_i are the values obtained by the optimization procedure ($Cost_{as}$, *TYPE*, d_{asb}, d_b + d_{sb}). The prediction models are often subject to the problem of overfitting. However, in this simple prediction model, it can be seen that the training and checking errors are comparable, which means that there is no overfitting. It should be noted that the main objective of this prediction model is to find the inputs that have the greatest impact on the output, not to build the prediction model with minimum training error. To achieve a higher accuracy in the prediction model, more neurons should be included in the neural networks, but this increase in neurons could lead to an overfitting problem.

Table 5
Optimal designs of pavement structures with depth of frost penetration h_m = 100 cm and site conditions f_{fr} = 0.8.

TYPE	T_n (–)	CBR (%)	h_m (cm)	f_{fr} (–)	d_{asb} (cm)	d_{as} (cm)	d_{ab} (cm)	d_b (cm)	d_{sb} (cm)	$COST_{as}$ (€/m^2)
B1U2(R)	1.0E + 04	3	100	0.8	8	0	8	27	55	58.62
B1U2(R)	1.0E + 05	3	100	0.8	8	0	8	27	55	58.62
B2U2(R)	1.0E + 06	3	100	0.8	13	4	9	26	51	67.3
B2U2(R)	1.0E + 07	3	100	0.8	22	4	18	28	40	83.38
B2U1(R)	1.0E + 08	3	100	0.8	36	4	32	54	0	111.14
B1U2	1.0E + 04	4	100	0.8	8	0	8	27	55	55.02
B1U2	1.0E + 05	4	100	0.8	8	0	8	27	55	55.02
B2U2	1.0E + 06	4	100	0.8	13	4	9	26	53	64.36
B2U2(R)	1.0E + 07	4	100	0.8	22	4	18	28	40	83.38
B2U2(R)	1.0E + 08	4	100	0.8	36	4	32	31	27	109.7
B1U2	1.0E + 04	5	100	0.8	8	0	8	27	55	55.02
B1U2	1.0E + 05	5	100	0.8	8	0	8	27	55	55.02
B2U2	1.0E + 06	5	100	0.8	13	4	9	26	51	63.7
B2U2	1.0E + 07	5	100	0.8	22	4	18	28	43	80.77
B2U2(R)	1.0E + 08	5	100	0.8	36	4	32	31	23	108.38
B1U2	1.0E + 04	6	100	0.8	8	0	8	27	55	55.02
B1U2	1.0E + 05	6	100	0.8	8	0	8	27	55	55.02
B2U2	1.0E + 06	6	100	0.8	13	4	9	26	51	63.7
B2U2	1.0E + 07	6	100	0.8	22	4	18	28	40	79.78
B2U2(R)	1.0E + 08	6	100	0.8	36	4	32	31	23	108.38
B1U2	1.0E + 04	7	100	0.8	8	0	8	27	55	55.02
B1U2	1.0E + 05	7	100	0.8	8	0	8	27	55	55.02
B2U2	1.0E + 06	7	100	0.8	13	4	9	26	51	63.7
B2U2	1.0E + 07	7	100	0.8	22	4	18	28	40	79.78
B2U2	1.0E + 08	7	100	0.8	36	4	32	31	28	106.43

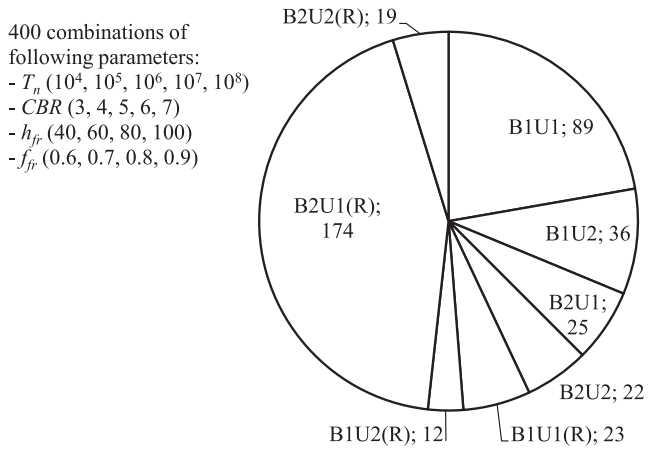

Fig. 5. Proportion of optimal pavement types among 400 defined parameter combinations.

It also examines the combination of two inputs that have the greatest influence on the output. The result of the parametric analysis clearly shows that the most important parameter for the optimal cost of a pavement structure is the total number of ESALs (T_n). This is followed by the equally important depth of frost penetration (h_m), site conditions (f_{fr}) and California Bearing Ratio (CBR).

The total number of ESALs is also most relevant for determining the optimal type of pavements and thicknesses of the asphalt layer, while the depth of frost penetration is most relevant to the total thickness of the unbound layers. The parametric analysis also shows that the "total number of ESALs" and the "depth of frost penetration" form the optimal combination of two inputs that are most relevant to the optimal cost: the optimal pavement type structure and the optimal thickness of the asphalt layer. However, the combination of "depth of frost penetration" and "hydrologic conditions at the site" is most relevant for determining the total thickness of the unbound layers.

5. Case study

To illustrate the usefulness of the optimization model presented in this article, an example is given for determining the cheapest possible pavement structure and finding an optimal design for the given design parameters. The design data are based on practical design project of road near village Sv. Ana, Slovenia [34]. The subgrade strength was determined from 15 CBR tests and the mean value of the CBR for a 3 km section of road was determined to be 4.3%. The total daily equivalent traffic-load in the cross section of

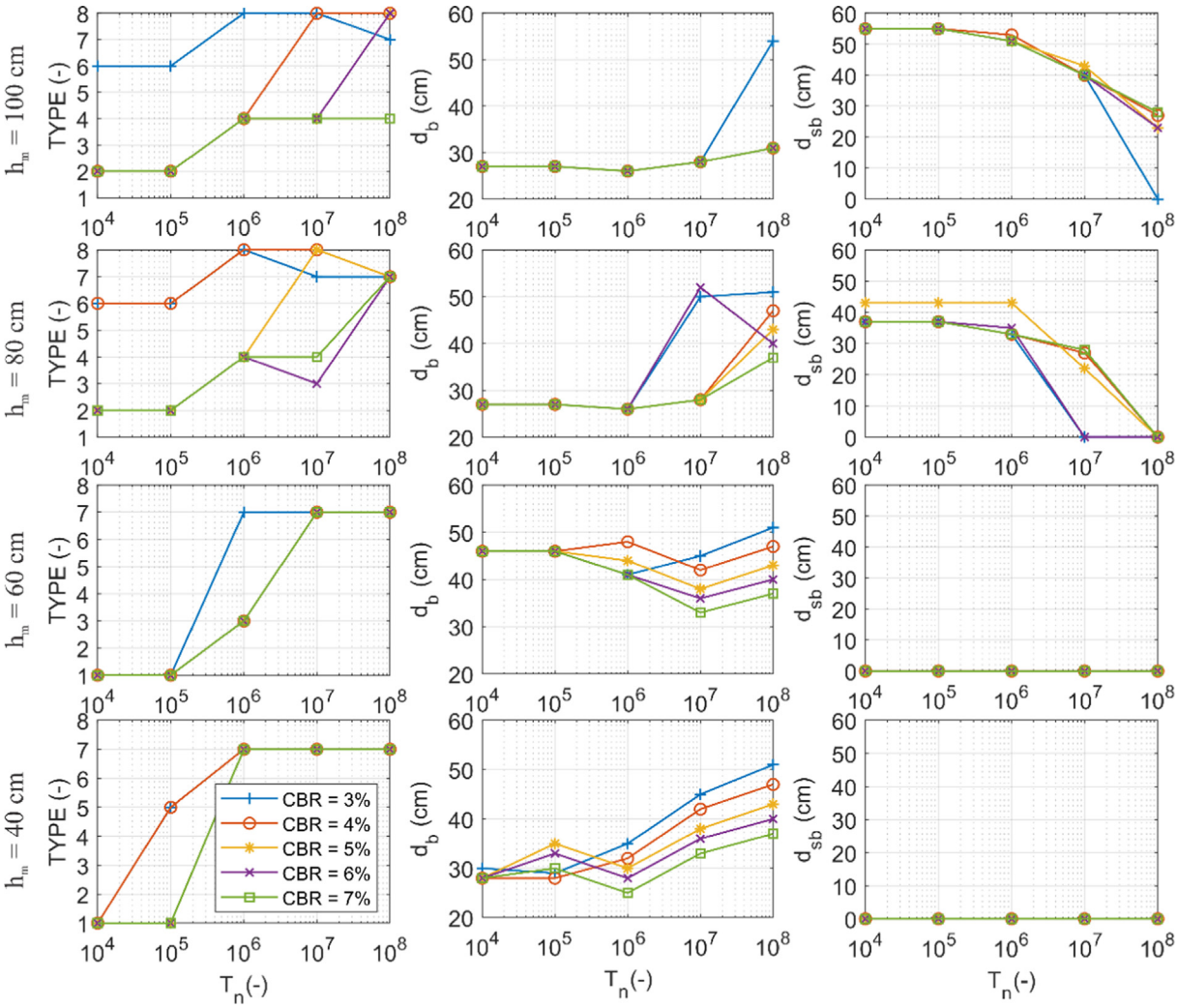

Fig. 6. Optimal pavement types and the thickness of layers for very unfavorable site conditions (f_{fr} = 0.9).

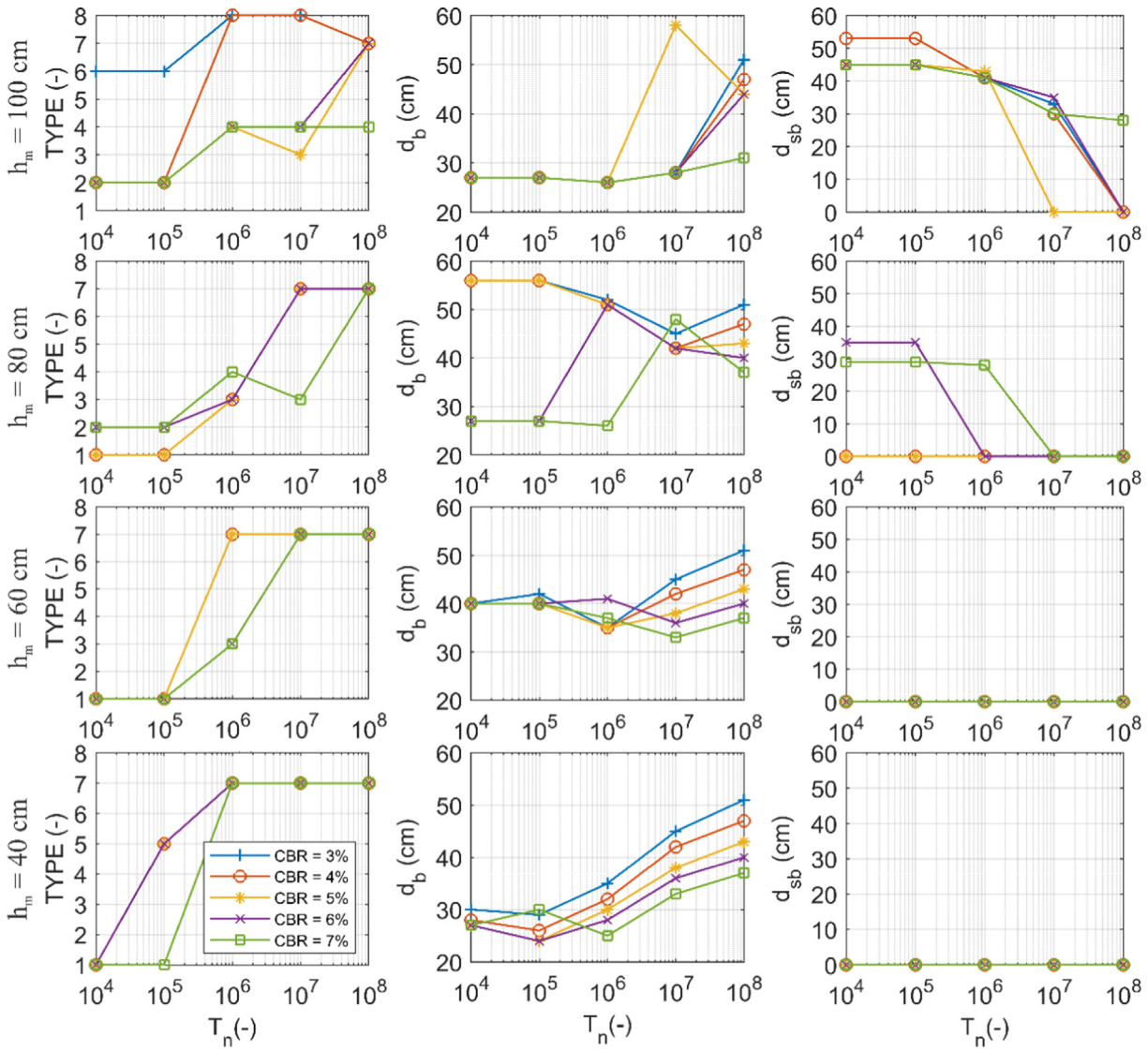

Fig. 7. Optimal pavement types and the thickness of layers for very unfavorable site conditions (f_{fr} = 0.8).

the pavement T_d was determined on the basis of the planned average daily number of motor vehicles in the first year of the pavement. The total number of ESALs $T_n = 2.56 \cdot 10^6$ was calculated by considering the total daily equivalent traffic load, the number of traffic lanes, lane widths, the longitudinal inclination of the pavement, additional dynamic impacts and the increasing traffic load due to traffic growth over its lifetime (n = 20 years). This calculation was performed using local technical specifications for roads [25] based on AASHTO [29] and European guidelines. The design data requires the depth of frost penetration h_m = 80 cm, unfavorable site conditions f_{fr} = 0.7, the width of the pavement structure covered with an asphalt layer B_{as} = 7 m, the width of the verge B_{ve} = 1 m and the length of the road section L = 3 km. All the other data involved in the optimization model were adopted from Table 3.

The results show that the optimal pavement structure for the given project data leads to a self-manufacturing cost of about 463.62 €/m, while the whole road section of 3 km costs 1.39 million €. The degree of utilization of each condition shows (see Table 8) that for the optimum design of the pavement structure for the selected example, all constraints have been fully utilized.

The results show that the optimal pavement structure for the given design data is the pavement structure type B2U1 (R). Due to the low CBR value of 4.3%, an engineer would intuitively choose a pavement structure consisting of an unbound sub-base layer to increase the CBR value of the ground, but the results show that such a pavement structure is not optimal. The material and construction costs are 463.62 €/m for the optimal pavement type and are 17% lower than if the engineer chose design type B1U2. The utilization ratio for pavement thickness-index and frost resistance shows that at least one of the conditions is almost fully utilized and a compromise must be found between the frost resistance and pavement thickness-index. Although the B1U1 (R) design type provides better utilization of the pavement thickness-index and frost resistance conditions, the price of a single-layer asphalt pavement proves to be less cost-effective in this case study. The percentage of cost difference Δ (%) shows the importance of choosing the right pavement type, even though each pavement type was subjected to optimization.

Table 6
Optimal pavement types with the cost and thickness of layers for favorable site conditions. (f_{fr} = 0.7).

f_{fr} = 0.7		h_m = 100 cm			h_m = 80 cm			h_m = 60 cm			h_m = 60 cm		
CBR (%)	T_n (–)	Type (–)*	d_b (cm)	d_{sb} (cm)	Type (–)*	d_b (cm)	d_{sb} (cm)	Type (–)*	d_b (cm)	d_{sb} (cm)	Type (–)*	d_b (cm)	d_{sb} (cm)
3	1.0E + 04	6	27	35	1	48	0	1	34	0	5	21	0
	1.0E + 05	6	27	35	1	48	0	1	42	0	5	29	0
	1.0E + 06	3	57	0	7	43	0	7	35	0	7	35	0
	1.0E + 07	7	48	0	7	45	0	7	45	0	7	45	0
	1.0E + 08	7	51	0	7	51	0	7	51	0	7	51	0
4	1.0E + 04	6	27	35	1	48	0	1	34	0	1	28	0
	1.0E + 05	6	27	35	1	48	0	1	38	0	5	26	0
	1.0E + 06	8	26	31	3	48	0	7	32	0	7	32	0
	1.0E + 07	8	28	27	7	42	0	7	42	0	7	42	0
	1.0E + 08	7	47	0	7	47	0	7	47	0	7	47	0
5	1.0E + 04	2	27	43	1	48	0	1	34	0	1	27	0
	1.0E + 05	2	27	43	1	48	0	1	35	0	5	24	0
	1.0E + 06	8	26	31	3	44	0	7	30	0	7	30	0
	1.0E + 07	8	28	21	7	38	0	7	38	0	7	38	0
	1.0E + 08	7	43	0	7	43	0	7	43	0	7	43	0
6	1.0E + 04	2	27	35	1	48	0	1	34	0	1	21	0
	1.0E + 05	2	27	35	1	48	0	1	42	0	5	29	0
	1.0E + 06	4	26	35	3	43	0	7	35	0	7	35	0
	1.0E + 07	8	28	20	7	36	0	7	45	0	7	45	0
	1.0E + 08	7	40	0	7	40	0	7	51	0	7	51	0
7	1.0E + 04	2	27	35	2	27	28	1	34	0	1	21	0
	1.0E + 05	2	27	35	2	27	28	1	34	0	5	29	0
	1.0E + 06	4	26	31	3	43	0	7	29	0	7	35	0
	1.0E + 07	3	48	0	7	34	0	7	33	0	7	45	0
	1.0E + 08	7	37	0	7	37	0	7	37	0	7	51	0

* 1 = B1U1, 2 = B1U2, 3 = B2U1, 4 = B2U2, 5 = B1U1(R), 6 = B1U2(R), 7 = B2U1(R), 8 = B2U2(R).

Table 7
Optimal pavement types with the cost and thickness of layers for very favorable site conditions. (f_{fr} = 0.6).

f_{fr} = 0.6		h_m = 100 cm			h_m = 80 cm			h_m = 60 cm			h_m = 40 cm		
CBR (%)	T_n (–)	Type (–)*	d_b (cm)	d_{sb} (cm)	Type (–)*	d_b (cm)	d_{sb} (cm)	Type (–)*	d_b (cm)	d_{sb} (cm)	Type (–)*	d_b (cm)	d_{sb} (cm)
3	1.0E + 04	1	52	0	1	40	0	1	30	0	5	21	0
	1.0E + 05	1	52	0	1	42	0	5	29	0	5	29	0
	1.0E + 06	3	52	0	7	35	0	7	35	0	7	35	0
	1.0E + 07	7	45	0	7	45	0	7	45	0	7	45	0
	1.0E + 08	7	51	0	7	51	0	7	51	0	7	51	0
4	1.0E + 04	1	52	0	1	40	0	1	28	0	5	21	0
	1.0E + 05	1	52	0	1	40	0	5	28	0	5	29	0
	1.0E + 06	3	48	0	7	35	0	7	32	0	7	35	0
	1.0E + 07	7	42	0	7	42	0	7	42	0	7	45	0
	1.0E + 08	7	47	0	7	47	0	7	47	0	7	51	0
5	1.0E + 04	1	52	0	1	40	0	1	28	0	1	27	0
	1.0E + 05	1	52	0	1	40	0	1	35	0	5	24	0
	1.0E + 06	3	47	0	7	35	0	7	30	0	7	30	0
	1.0E + 07	7	38	0	7	38	0	7	38	0	7	38	0
	1.0E + 08	7	43	0	7	43	0	7	43	0	7	43	0
6	1.0E + 04	1	52	0	1	40	0	1	30	0	5	21	0
	1.0E + 05	1	52	0	1	40	0	1	29	0	5	29	0
	1.0E + 06	3	47	0	3	41	0	7	35	0	7	35	0
	1.0E + 07	7	38	0	7	36	0	7	45	0	7	45	0
	1.0E + 08	7	40	0	7	40	0	7	51	0	7	51	0
7	1.0E + 04	2	27	28	1	40	0	1	28	0	5	21	0
	1.0E + 05	2	27	28	1	40	0	1	30	0	5	29	0
	1.0E + 06	4	26	28	3	37	0	7	25	0	7	35	0
	1.0E + 07	7	38	0	7	33	0	7	33	0	7	45	0
	1.0E + 08	7	37	0	7	37	0	7	37	0	7	51	0

* 1 = B1U1, 2 = B1U2, 3 = B2U1, 4 = B2U2, 5 = B1U1(R), 6 = B1U2(R), 7 = B2U1(R), 8 = B2U2(R).

6. Conclusion

Optimizations were performed 3200 times to obtain an optimal pavement design for different ESALs, CBR, depth of frost penetrations and site conditions (materials and hydrology). The results of this study provide engineers with important information on what type of pavement to select for different project data to minimize pavement construction costs. Since the optimization model was developed in a general form, engineers can assign their own values to the terms in the equations to adapt the parameters to their specific site conditions and economic environment. The results of the study allow a direct comparison between geosynthetically reinforced and unreinforced flexible pavement structures once they are optimized. The following conclusions can be

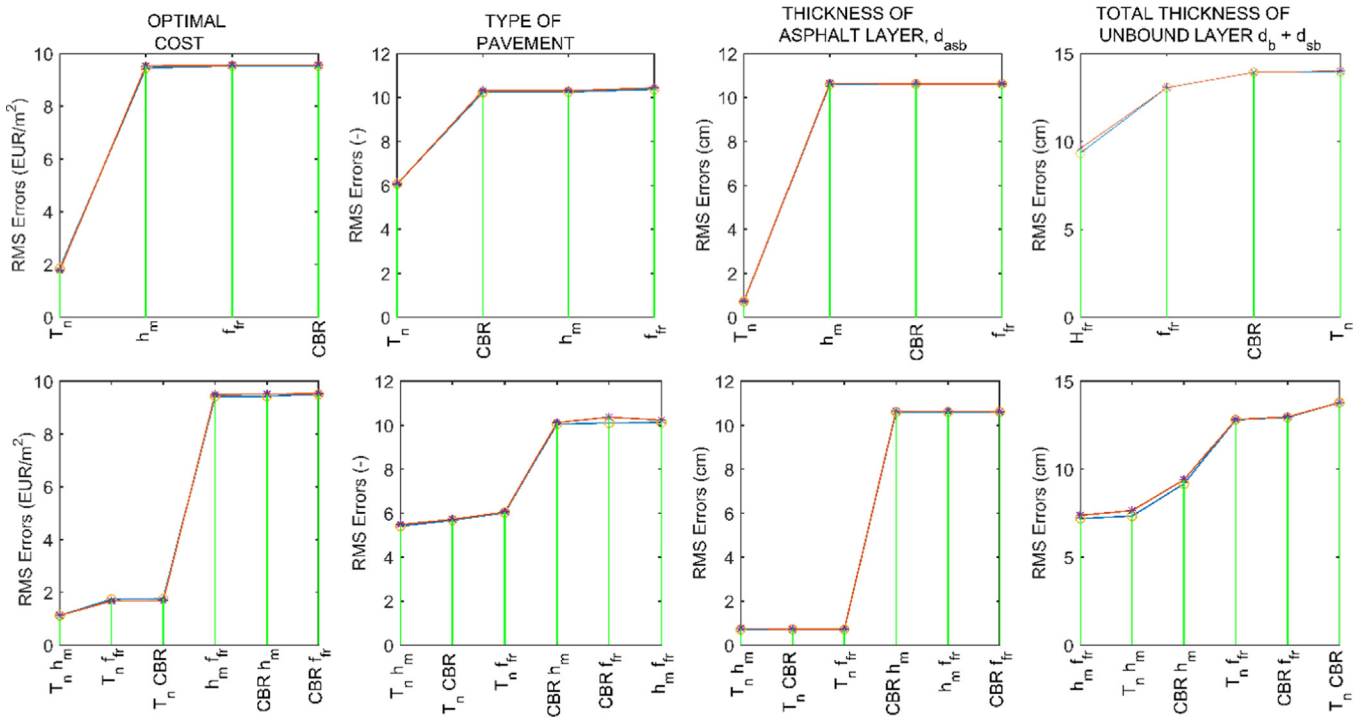

Fig. 8. Influence of each input variable on the optimal cost of a pavement structure and the utilization of geotechnical conditions.

Table 8
Optimal design of a pavement structure – case study.

TYPE	d_{asb} (cm)	d_{as} (cm)	d_{ab} (cm)	d_b (cm)	d_{sb} (cm)	D_{total}/D_{req} (%)	h_{total}/h_{req} (%)	*COST* (€/m')	Δ (%)
B1U1	16	0	0	54	0	99	80	516.42	10.2
B1U2	16	0	0	29	25	99	59	558.42	17.0
B2U1	0	4	12	52	0	99	82	481.22	3.7
B2U2	0	4	12	27	50	99	60	523.22	11.4
B1U1 (R)	16	0	0	40	0	96	100	491.62	5.7
B1U2 (R)	16	0	0	29	25	99	80	518.02	10.5
B2U1 (R)	0	4	12	40	0	93	100	**463.62**	0.0
B2U2 (R)	0	4	12	27	25	99	82	482.82	4.0

drawn from the performed multiparametric optimization based on 3200 optimized pavement designs:

- For lower CBR values (up to 4%), pavement designs with geosynthetic reinforcement predominate as the optimal solution. The cost of geosynthetic reinforcement has been shown to be less expensive than a thicker unbound base course or unbound sub-base due to savings in material volume and excavation.
- Geosynthetic reinforcement also allows for more cost-effective pavement designs at higher ESALs (greater than $1 \cdot 10^7$ ESAL).
- Flexible pavements reinforced with geosynthetics are a more cost-effective solution, especially when site conditions are favorable (f_{fr} = 0.6/0.7) with frost resistant materials, good hydrological conditions and with a thickness of the pavement structure that is determined by the pavement thickness-index rather than the required frost depth. At shallower frost depths (h_m = 40 cm, 60 cm), the required total thickness of the base and sub-base layers decreases and the pavement thickness-index becomes a critical factor in pavement design, favoring the use of geosynthetic reinforcement.
- The sensitivity analysis showed that the most important parameter for the optimal cost of a pavement design are ESALs (T_n). The ESALs (T_n) are also the most important parameter in determining the asphalt layer thickness and the type of pavement design. Only the thickness of the unbound layer thickness is governed by the frost penetration depth (h_m).
- The combination of ESALs and frost penetration depth has the greatest influence on optimum cost, type of pavement design and asphalt layer thickness. The total thickness of the unbound layer is mainly influenced by the combination of frost penetration depth and site conditions (materials, frost resistance and hydrological conditions).
- The parametric study also revealed that at the most unfavorable design parameters, the optimal cost of the pavement was 133.87 €/m^2, while for the most favorable design parameters it was 36.87 €/m^2.
- The case study results show that selecting the optimal pavement type reduces pavement costs by 17%, even though each pavement type was subjected to optimization.

The current study is based on an empirical method for pavement design. However, an improved optimization model based on mechanical-empirical (M–E) design methods should be developed that can accurately represent the stress–strain formation in the pavement layers and geosynthetic reinforcement. While this study only considers the optimization of pavement construction

costs, the objective function can also be extended to the carbon footprint.

Declaration of Competing Interest

The authors declare that they have no known competing financial interests or personal relationships that could have appeared to influence the work reported in this paper.

Acknowledgments

This research was funded by the Slovenian Research Agency (grant number P2-0268) and the GEOLAB project (grant number 101006512).

References

[1] Zornberg JG. Advances in the use of geosynthetics in pavement projects. Geosintec Iberia 2015; 2: 1–13.
[2] Rouphail NM. Minimum-Cost Design of Flexible Pavements. J Transp Eng 1985;111(3):196–207. doi: https://doi.org/10.1061/(ASCE)0733-947X(1985)111:3(196).
[3] Nicholls R. Optimization of AASHTO DNPS86 pavement design program. J Transp Eng 1991;117(2):189–209. doi: https://doi.org/10.1061/(ASCE)0733-947X(1991)117:2(189).
[4] Hadi MNS, Arfiadi Y. Optimum rigid pavement design by genetic algorithms. Comput Struct 2001;79(17):1617–24. doi: https://doi.org/10.1016/S0045-7949(01)00038-4.
[5] Pryke A, Evdorides H, Ermaileh RA. Optimization of pavement design using a genetic algorithm. In: 2006 IEEE Congr Evol Comput CEC 2006; 2006, p. 1095–8.
[6] Gaurav, Wojtkiewicz SF, Khazanovich L. Optimal design of flexible pavements using a framework of DAKOTA and MEPDG. Int J Pavement Eng 2011;12 (2):137–48. doi: https://doi.org/10.1080/10298436.2010.535535.
[7] Ghanizadeh AR. An Optimization Model for Design of Asphalt Pavements Based on IHAP Code Number 234. Adv Civ Eng 2016;2016:1–8. doi: https://doi.org/10.1155/2016/5942342.
[8] Tohidi M, Khayat N, Telvari A. The use of intelligent search algorithms in the cost optimization of road pavement thickness design. Ain Shams Eng J 2022;13 (3):101596. doi: https://doi.org/10.1016/j.asej.2021.09.023.
[9] Mamlouk MS, Zaniewski JP, He W. Analysis and design optimization of flexible pavement. J Transp Eng 2000;126(2):161–7. doi: https://doi.org/10.1061/(ASCE)0733-947X(2000)126:2(161).
[10] Santos J, Ferreira A. Pavement Design Optimization Considering Costs and Preventive Interventions. J Transp Eng 2012;138(7):911–23. doi: https://doi.org/10.1061/(ASCE)TE.1943-5436.0000390.
[11] Madanat S, Prozzi JA, Han M. Effect of Performance Model Accuracy on Optimal Pavement Design. Comput Civ Infrastruct Eng 2002;17(1):22–30. doi: https://doi.org/10.1111/1467-8667.00249.
[12] Abaza KA, Abu-Eisheh† SA. An Optimum Design Approach for Flexible Pavements. Int J Pavement Eng 2003;4(1):1–11. doi: https://doi.org/10.1080/1029843031000087464.
[13] Tarefder RA, Bateman D. Design of Optimal Perpetual Pavement Structure. J Transp Eng 2012;138(2):157–75. doi: https://doi.org/10.1061/(ASCE)TE.1943-5436.0000259.
[14] McDonald M, Madanat S. Life-Cycle Cost Minimization and Sensitivity Analysis for Mechanistic-Empirical Pavement Design. J Transp Eng 2012;138 (6):706–13. doi: https://doi.org/10.1061/(ASCE)TE.1943-5436.0000346.
[15] Zhang H, Keoleian GA, Lepech MD, Kendall A. Life-Cycle Optimization of Pavement Overlay Systems. J Infrastruct Syst 2010;16(4):310–22. doi: https://doi.org/10.1061/(ASCE)IS.1943-555X.0000042.
[16] Lee SI, Carrasco G, Mahmoud E, Walubita LF. Alternative Structure and Material Designs for Cost-Effective Perpetual Pavements in Texas. J Transp Eng Part B Pavements 2020;146(4):04020071. doi: https://doi.org/10.1061/JPEODX.0000226.
[17] Sanchez-Cotte EH, Fuentes L, Martinez-Arguelles G, Rondón Quintana HA, Walubita LF, Cantero-Durango JM. Influence of recycled concrete aggregates from different sources in hot mix asphalt design. Constr Build Mater 2020;259:120427. doi: https://doi.org/10.1016/j.conbuildmat.2020.120427.
[18] Mamlouk* MS, Zaniewski† JP. Optimizing Pavement Preservation: An Urgent Demand for Every Highway Agency. Int J Pavement Eng 2001;2(2):135–48. doi: https://doi.org/10.1080/10298430108901722.
[19] Chong D, Wang Y, Dai Z, Chen X, Wang D, Oeser M. Multiobjective optimization of asphalt pavement design and maintenance decisions based on sustainability principles and mechanistic-empirical pavement analysis. Int J Sustain Transp 2018;12(6):461–72. doi: https://doi.org/10.1080/15568318.2017.1392657.
[20] Walubita LF, Jamison BP, Das G, Scullion T, Martin AE, Rand D, et al. Search for a Laboratory Test to Evaluate Crack Resistance of Hot-Mix Asphalt. Transp Res Rec J Transp Res Board 2011;2210(1):73–80. doi: https://doi.org/10.3141/2210-08.
[21] Walubita LF, Mahmoud E, Lee SI, Carrasco G, Komba JJ, Fuentes L, et al. Use of grid reinforcement in HMA overlays – A Texas field case study of highway US 59 in Atlanta District. Constr Build Mater 2019;213:325–36. doi: https://doi.org/10.1016/j.conbuildmat.2019.04.072.
[22] Sanchez-Silva M, Arroyo O, Junca M, Caro S, Caicedo B. Reliability based design optimization of asphalt pavements. Int J Pavement Eng 2005;6(4):281–94. doi: https://doi.org/10.1080/10298430500445506.
[23] Rajbongshi P, Das A. Optimal Asphalt Pavement Design Considering Cost and Reliability. J Transp Eng 2008;134(6):255–61. doi: https://doi.org/10.1061/(ASCE)0733-947X(2008)134:6(255).
[24] Saride S, Peddinti PRT, Basha MB. Reliability Perspective on Optimum Design of Flexible Pavements for Fatigue and Rutting Performance. J Transp Eng Part B Pavements 2019;145(2):04019008. doi: https://doi.org/10.1061/JPEODX.0000108.
[25] TSC 06.520:2009. PROJEKTIRANJE DIMENZIONIRANJE NOVIH ASFALTNIH VOZIŠCNIH KONSTRUKCIJ; 2009.
[26] MATLAB-MathWorks; 2020.
[27] Deep K, Singh KP, Kansal ML, Mohan C. A real coded genetic algorithm for solving integer and mixed integer optimization problems. Appl Math Comput 2009;212(2):505–18. doi: https://doi.org/10.1016/j.amc.2009.02.044.
[28] Walubita LF, Lee SI, Faruk ANM, Hoeffner J, Scullion T, Abdallah I, et al. Texas Flexible Pavements and Overlays: Calibration Plans for M-E Models and Related Software. Texas Dep Transp Fed Highw Adm Rep FHWA/TX-13/0-6658-P4 2013; 7: 146.
[29] Aashto. AASHTO Guide for Design of Pavement Structures. Am Assoc State Highw Transp Off 1993.
[30] Giroud JP, Han J. Design Method for Geogrid-Reinforced Unpaved Roads. I. Development of Design Method. J Geotech Geoenvironmental Eng 2004;130 (8):775–86. doi: https://doi.org/10.1061/(ASCE)1090-0241(2004)130:8(775).
[31] Giroud JP, Han J. Design Method for Geogrid-Reinforced Unpaved Roads. II Calibration and Applications. J Geotech Geoenviron Eng 2004;130(8):787–97. doi: https://doi.org/10.1061/(ASCE)1090-0241(2004)130:8(787).
[32] Geosynthetics T, America N. Flexible Pavement Design using TenCate Mirafi ® Geosynthetics. Tencate Des Guidel 2014:1–7. https://www.tencategeo.us/media/12b6acdd-f429-4af4-8298-34337d1ad693/2xEilA/TenCate Geosynthetics/Documents AMER/Design Guidelines/DG_flexible pavement.pdf.
[33] Meyer N, Elias JM. Design Methods for Roads Reinforced with Multifunctional Geogrid Composites for Subbase Stabilization. Kunststoff 1999.
[34] Žlender B. Reconstruction of the road R3-730/4104 Žice - Sveta Ana - Zgornja Ščavnica; section 4104 Žice - Sveta Ana - Zgornja Ščavnica; from km 0.000 to 2.489 2020. https://plus.cobiss.net/cobiss/si/en/bib/101057027?lang=en.

Dr. Primož Jelušič is associate professor at the Faculty of Civil Engineering, Transportation Engineering and Architecture, University of Maribor, Slovenia. He started his career 2005 when he obtained his diploma at the Faculty of Civil Engineering, Maribor (2009). Primož Jelušič obtained his PhD in 2013 at the Faculty of Civil Engineering, University of Maribor, where he was employed as assistant in the field of Building Materials an assistant in the field of Geotechnics. Associate prof. dr. Primož Jelušič is involved in pedagogical and research work at the University of Maribor, Faculty of Civil Engineering, Traffic Engineering and Architecture. His research is primarily focused on the optimization of structures and Geotechnics. Dr. Primož Jelušič constantly transfers gained knowledge into practice, through the education of students at home and abroad. He recommended optimal design for a piled embankment's, reinforced earth structures, retaining walls, underground gas storages, geothermal energy piles, shallow foundations and other widely used civil engineering structures. These civil and geotechnical engineering structures improve mobility and competitiveness of European region. Primož task is also to carry out the revision of civil engineering projects important for the community. Primož research group at University of Maribor was engaged in projects with a number of industrial partners and Slovenian municipalities.